

PAPER • OPEN ACCESS

Structural and Optical Properties of Si Nanostructures

To cite this article: Ashish Kumar *et al* 2019 *IOP Conf. Ser.: Mater. Sci. Eng.* **594** 012001

View the [article online](#) for updates and enhancements.

Structural and Optical Properties of Si Nanostructures

Ashish Kumar^{1*}, Ashok Sharma¹, and Ajay Agarwal¹

¹CSIR-Central Electronics Engineering Research Institute, Pilani, 333031, Rajasthan India

*Email: ashishvlsi10@gmail.com

Abstract: Silicon nanostructures were realized using metal assisted chemical etching of silicon wafer (100) for two different etching times: 5 minute and 10 minute. Structural and optical properties of silicon nanostructures were investigated using field emission scanning electron microscopy (FESEM), X-ray diffraction (XRD), and photoluminescence (PL). XRD analysis probes the changes in crystallinity during etching and reveals reflection plane (220) of obtained silicon nanostructures. UV and visible spectra of photoluminescence from Si nanostructures suggest the optically active nature of Si at nanoscale and confinement of carrier. These results show that the structural and optical properties of Si nanostructures strongly depend on etching time of silicon wafer.

Keywords: MACE; Silicon nanostructures; and Quantum confinement

1. Introduction: The famous lecture “There's Plenty of Room at the Bottom: An Invitation to Enter a New Field of Physics” of Richard Feynman in 1959 promoted research community to harvest the unique and structural properties of materials at nanoscale which are absent in bulk structures [1]. However, the visions of Richard Feynman came into the reality with the advancement in technology in the early decade of 21 century. Since then, research community have demonstrated numerous nanostructures of various materials such as Si, ZnO, SnO₂ and etc. to study unique properties of material at nanoscale [2]. Among all these material, silicon is more attractive for nanoelectronics application as well documented properties and easy integration with exciting technology are addition advantage of Si nanostructures (NSs) over other materials [3-6]. Since the first report of Si NSs in 1950 by Uhler [3], Si NSs with control morphology demonstrated potential application in the fields ranging from electronic, sensor, energy storage, flexible electronics photovoltaics, and energy storage electrodes [4-5]. However, with an indirect band gap material Si NSs can hardly be explored for optoelectronic application till the discovery of luminescent in Si NSs due to carrier confinement. Optically active nature of Si NSs or porous Si has attracted significant attention to demonstrate efficient and cost effective light emitting diode and laser.

Despite the various application of Si NSs, current fabrication methods reactive ion etching, other dry etching which are commonly used for micro nanofabrication are not suitable for mass production of Si NSs at large scale with high aspect ratios [4]. With the advancement in catalyst chemistry, an alternative approach metal assist chemical etching (MACE) has attracted a great interest to develop Si NSs because of its simplicity; low cost, and versatility [6-7]. Various types of Si NSs i. e. Si nanowires, porous Si from many type of Si wafer (100) and Si(111) with different doping levels p-type Si or n-type Si wafers, have been demonstrated using this method. The MACE process begins with partial coating of metal nanoparticles over Si surface followed by etching of Si in acidic oxidizing solution of hydrogen peroxide (H₂O₂) and hydrofluoric acid (HF). Here metal nanoparticles works catalyst and enhance the etch rate of Si beneath of NPs. Although realization of Si NSs using MACE is very easy and significant effort have been made to explain etching mechanism of Si in the presence of metal NPs, structural and luminescent properties of Si NSs are yet to address. ,



In this work, we reported the development of vertically aligned Si NSs through etching of lightly doped Si wafer utilizing gold (Au) NPs in MACE process. XRD analysis of silicon NSs showed the variations in the crystal lattice than its bulk wafer which might correspond to oxidation rate of crystal plane. Photoluminescence of Si NSs shows intense blue and red emission at room temperature attributed to quantum confinement carrier at nanoscale.

2. Experimental Procedures:

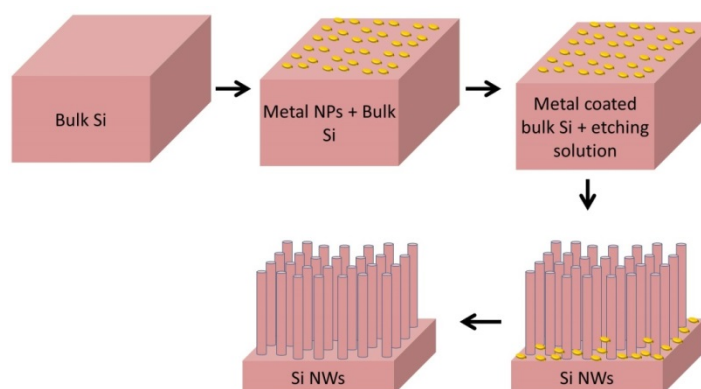


Fig. 1 Processes flow MACE for formation of Si Nanostructures

For experiment, single side polished p-type Si (100) wafers with resistivity (1-10) Ω -cm were considered. Si wafer were cleaned using standard degreasing and RCA cleaning process of semiconductor industry. Cleaned Si wafer were decorated with 10 nm thickness of gold (Au) metal nanoparticles (NPs) by e-beam evaporation system. Further, Au NPs coated wafers were immersed in etchant solution of H_2O_2 and HF (2:1) for 5 and 10 minutes. After developing process, substrates were dipped in etchant solution of Au to remove metal NPs from the Si NSs and followed by bath of NSs in HF solution to remove oxide layer which was produced in Au etchant solution. The process flow for the development of Si NSs figure 1. For further simplicity in discussion, we named the sample S1 and S2 of Si NSs which were obtained by different etching time duration 5 and 10 minutes respectively. Crystal properties of etched wafers were characterized by Powder XRD (Rigaku Smart Lab system® with Cu-K α radiation operating at 40 kV and 40 mA, with wavelength (λ) = 1.5418 Å. FESEM reveals surface morphology of textured surface of samples. Photoluminescence spectra of samples was recorded with high power 325 nm He-Cd laser excitation power source using Dongwoo optron 80K PL system at room temperature.

3. Results and Discussion:

Textured surface of Si wafer was revealed in FESEM images and shown in the figure 2 (a-b) for sample S1 and S2. Though, surface profile of etched wafer is quite smiler. Etch depth of silicon was not same for different etching time as revealed in cross section images 2(c-d). Etching depth of sample S1 was recorded 22 μm while 33 μm for sample S2. Cross section images exhibited uniform distribution of dense and isolated Si NSs on entire sample. Long NSs as shown in the figures confirmed that MACE process is capable to produce high aspect ratio NSs in less time than dry reactive ion etching process. Vertical alignment of Si NSs shows that electrochemical reaction of HF and H_2O_2 took place at the interface of Si and Au NPs. Au NPs works as catalyst and enhance the anisotropic etching of Si. The electrochemical reaction is similar to two electrode configuration under galvanostatic control. Here Si substrate works as the anode electrode and metal NPs works cathode electrode. During the reaction Si atoms are oxidized in the presence of HF and removed from the surface as intermediate products SiF_4 or SiF_6^{2-} are soluble in water. During the reaction Si atom released electron and oxidize after adsorption of hole. The released electrons are capture by Au NPs. The various chemical reactions have been proposed to describe the MACE analogous anodic etching of Si in HF [5-6].

It is well established that H_2O_2 is reduced at the metal (cathode) and generate hole



Generated hole is adsorbed by Si surface and leads oxidation of Si and followed by dissolution of oxide



Since the reaction take place at the surface of Si, surface states of Si also play an important role to control the morphology of etched Si. Up to now, the role of surface states in the metal assisted chemical etching is not explored. Moreover, morphology of Si NSs i. e. the length, diameter, and interface are strongly functions of catalyst shape, size, concentration of HF and H_2O_2 and etching time.

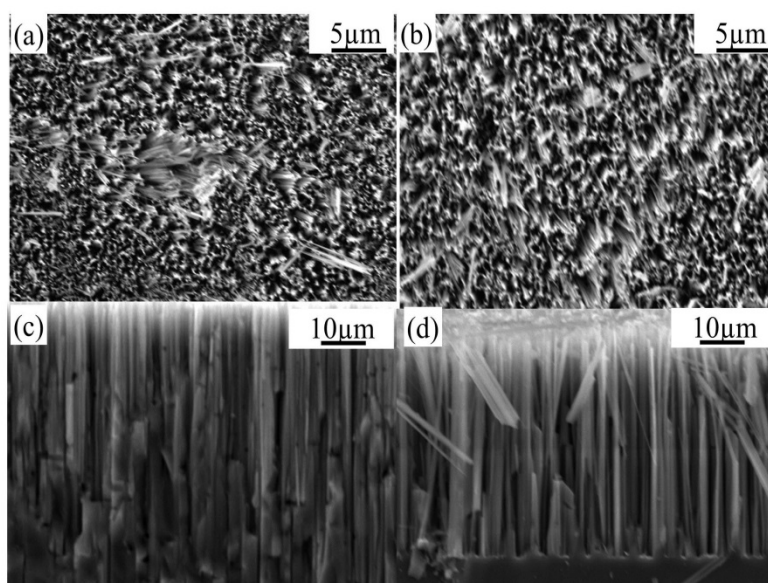


Fig. 2 FESEM images of silicon nanostructures obtain after etching of Si wafer for (a) 5 minutes and (b) 10 minutes

In order to understand the crystal structures of etched Si NSs, XRD plots of the samples (S1 and S2) are presented in figure 3 (a-b) respectively. The common diffraction peak in both figures was observed at diffraction angle of 2θ (44.5°) and can be assigned to diffraction plane of silicon (220) [9]. A distinguish peak for the sample S1 at the value of 2θ (28.53°) is well assigned to Si (111) plane [9]. The presence of plane (111) indicates the Si atom is not etched in (111) direction [10]. The anisotropic etching of Si was described using the back bond breaking theory. According to this theory, bond of Si surface atom connect to underneath atom and break during oxidation and dissolution process of MACE. The stronger the back bond strength the more difficult to remove the atom. Bond strength of surface Si atom is decided by crystal orientation of substrate. Si atom on the surface of a (100) substrate has two back bonds while atom on (111) substrate has three back bond. Therefore, atom on (100) surface plane is easily etched than the atom present on plane (111). The similar result was observed for sample S1. As etching increases, only crystal orientation (220) of Si nanostructures was observed. Here it is worth to mention that etching of Si in MACE process is very

complicated. The detail etching mechanism of Si with respect to metal NPS is yet to explain. Other than diffraction peaks, a small hump was also observed at lower diffraction angle in both figures and indicated the oxidation of developed Si NSs in open environment. Full width half maximum (FWHM) also gives important information for the crystalline size: Large value of FWHM indicates smaller the crystal size. The values of FWHM corresponding to diffraction plane (220) was calculated via origin peak analyser and found 0.35° and 0.42° for the sample S1 and S2 respectively. Larger etching time produces small crystalline size and responsible for the large value of FWHM.

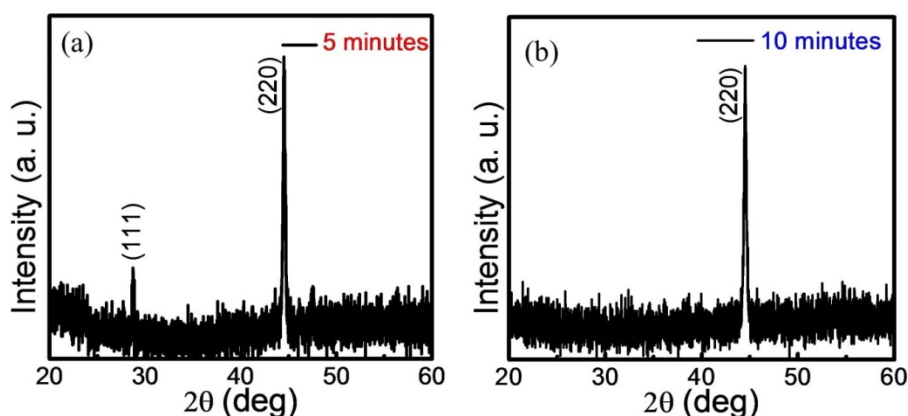


Fig. 3. XRD analysis of etched Si nanostructures obtain after etching of bulk Si wafer

Finally we investigated the luminescent properties of developed Si NSs. Strong luminescent spectra for both samples were recorded from the samples and shown in figures 4 (a-b). Si NSs exhibits visible emission at room temperature without any treatment of surface. However, emission spectrum at the wavelengths 620-650 for sample S1 in figure 4(a) was slightly different from emission spectra of sample S2 where only blue emission centred between 350-450 nm was observed in figure 4 (b). The image of room temperature emission of the samples were also captured and shown in the inset of graph corresponding to each sample. Visible emission of Si NSs is strongly depends on structural properties of Si NSs and therefore PL can provide the information about size or morphology present in samples. Multicolour emission covering entire visible spectra from individual Si nanowire is reported by K. Seo and his research group [11]. Therefore it is concluded that a range of diameters of Si NSs were present in the sample S1 as also confirmed in XRD analysis by the presence of (111) crystal plane. However, as the etching time increased, plane (111) dissolved and only single plane of NSs could be responsible for single peak of luminescent for sample S2. Additionally small particles sizes enhance carrier confinement and might be responsible for blue shift in emission. Here, small particles size could be achieved by long etching time i.e. 10 minutes for sample S₂. These results are similar to reported photoluminescence spectra of Si NWs produced in longer etching time corresponding to carrier confinement at Bohr radius ($\approx 5\text{nm}$) of Si NSs. However diameters range ($\approx 50\text{nm}$ to 100nm) of Si NSs in this experiment was measured using SEM within its resolution limit. Therefore, surface morphology of Si NSs could be responsible lower wavelength emission instead of quantum confinement of carrier. Origin of red emission is expected from the carrier confinement corresponding to bandgap of silicon. However the blue, orange-red emission is greater than the band gap of bulk Si can be assign to combine effect of carrier confinement and surface states. The present blue emission in the fabricated Si NSs could be attributed to low doping level of Si wafer and presence of dangling bond at the surface. A reasonable mechanism for explanation of luminescent in Si NSs is subject of debate.

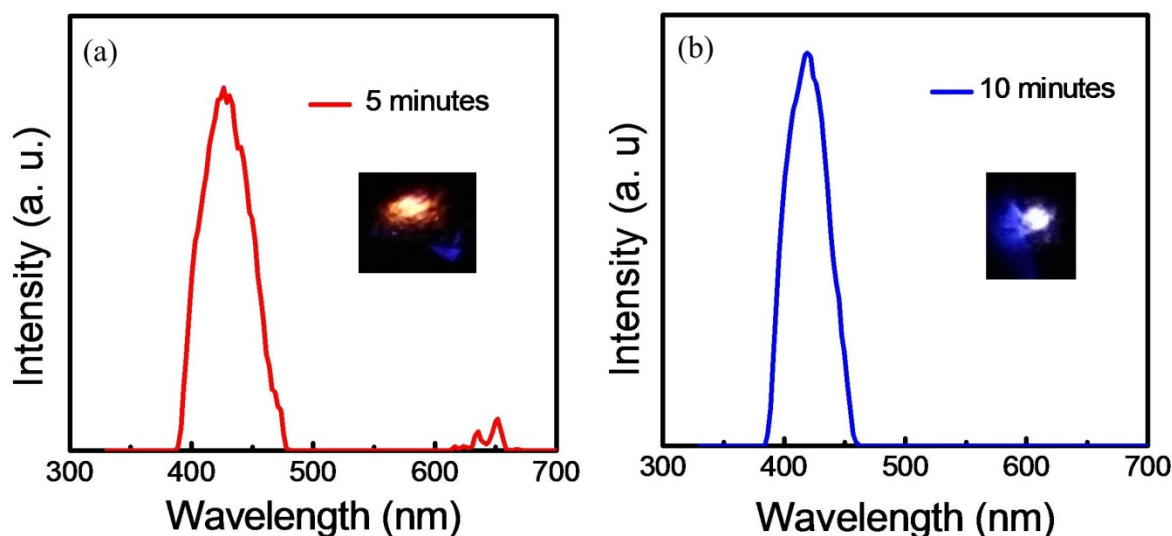


Fig. 4 Photoluminescence spectra of Si nanostructures obtain after etching of Si wafer for (a) 5 minutes and (b) 10 minutes

4. Conclusions: In summary, a facile and cost effective method of electroless chemical etching was described for the development of Si nanostructures from p-type Si wafer (100). We employed sputtering method for Au deposition on the Si surface. Crystalline properties of etched Si strongly depend on etching conditions: time, size of metal nanoparticles, and concentration of etchant solution. Si crystal plane (100) easily dissolved in etchant solution than the (111) plane. Etched Si also shows optically active nature i. e. luminescent in broad range blue to red emission corresponding to carrier confinement effect and surface defect. Thus presented work give brief overview of Si NSs formation and their properties; could be helpful for further probe and application of Si NSs for various application especially cost effective light emitting devices.

Acknowledgements: A. Kumar is also thankful to Director; CSIR-CERRI support to carry out this research work. Authors are also grateful to technical staff of CSIR-CEERI Pilani for their help during the experiment.

References:

- [1]. Feynman, R.P., 2012. There's plenty of room at the bottom: An invitation to enter a new field of physics. In *Handbook of Nanoscience, Engineering, and Technology*, Third Edition (pp. 26-35). CRC Press.
- [2]. Zhang, L. and Webster, T.J., 2009. Nanotechnology and nanomaterials: promises for improved tissue regeneration. *Nano today*, 4(1), pp.66-80.
- [3]. Osminkina, L. A., Gonchar, K. A., Marshov, V. S., Bunkov, K. V., Petrov, D. V., Golovan, L. A., & Timoshenko, V. Y. (2012). Optical properties of silicon nanowire arrays formed by metal-assisted chemical etching: evidences for light localization effect. *Nanoscale research letters*, 7(1), 524.
- [4]. Patil, J.J., Smith, B.D. and Grossman, J.C., 2017. Ultra-high aspect ratio functional nanoporous silicon via nucleated catalysts. *RSC Advances*, 7(19), pp.11537-11542.
- [5]. Huang, Z., Geyer, N., Werner, P., De Boer, J., & Gösele, U. (2011). Metal-assisted chemical etching of silicon: a review. *Advanced materials*, 23(2), 285-308.
- [6]. Han, H., Huang, Z. and Lee, W., 2014. Metal-assisted chemical etching of silicon and nanotechnology applications. *Nano today*, 9(3), pp.271-304.
- [7]. Toor, F., Miller, J.B., Davidson, L.M., Duan, W., Jura, M.P., Yim, J., Forziati, J. and Black, M.R., 2016. Metal assisted catalyzed etched (MACE) black Si: optics and device physics. *Nanoscale*, 8(34), pp.15448-15466.
- [8]. Zhang, Y. F., Tang, Y. H., Wang, N., Yu, D. P., Lee, C. S., Bello, I., & Lee, S. T. (1998). Silicon nanowires prepared by laser ablation at high temperature. *Applied physics letters*, 72(15), 1835-1837.
- [9]. Kim, J., Kim, Y. H., Choi, S. H., & Lee, W. (2011). Curved silicon nanowires with ribbon-like cross sections by metal-assisted chemical etching. *Acs Nano*, 5(6), 5242-5248.

- [10]. Huang, Z., Shimizu, T., Senz, S., Zhang, Z., Geyer, N. and Gosele, U., 2010. Oxidation rate effect on the direction of metal-assisted chemical and electrochemical etching of silicon. *The Journal of Physical Chemistry C*, 114(24), pp.10683-10690.
- [11]. Seo, K., Wober, M., Steinvurzel, P., Schonbrun, E., Dan, Y., Ellenbogen, T., & Crozier, K. B. (2011). Multicolored vertical silicon nanowires. *Nano letters*, 11(4), 1851-1856.